Hindawi
International Journal of Antennas and Propagation
Volume 2018, Article ID 3029152, 11 pages
https://doi.org/10.1155/2018/3029152

Research Article

Analysis of Heuristic Uniform Theory of Diffraction Coefficients for Electromagnetic Scattering Prediction

Diego Tami[1], **Cássio G. Rego**[1], **Dinael Guevara**[2], **Andrés Navarro**[3], **Fernando J. S. Moreira**[1], **Jordi Giménez**[4] and **Hernan G. Triana**[3]

[1]*Graduate Program in Electrical Engineering, Federal University of Minas Gerais, Belo Horizonte, MG, Brazil*
[2]*Francisco de Paula Santander University, Cúcuta, Colombia*
[3]*Universidad Icesi, Cali, Colombia*
[4]*Universitat Politècnica de Valencia, Valencia, Spain*

Correspondence should be addressed to Andrés Navarro; anavarro@icesi.edu.co

Received 26 July 2017; Revised 17 December 2017; Accepted 2 January 2018; Published 7 March 2018

Academic Editor: Ikmo Park

We discuss three sets of heuristic coefficients used in uniform theory of diffraction (UTD) to characterize the electromagnetic scattering in realistic urban scenarios and canonical examples of diffraction by lossy conducting wedges using the three sets of heuristic coefficients and the Malyuzhinets solution as reference model. We compare not only the results of the canonical models but also their implementation in real outdoor scenarios. To predict the coverage of mobile networks, we used propagation models for outdoor environments by using a 3D ray-tracing model based on a brute-force algorithm for ray launching and a propagation model based on image theory. To evaluate each set of coefficients, we analyzed the mean and standard deviation of the absolute error between estimates and measured data in Ottawa, Canada; Valencia, Spain; and Cali, Colombia. Finally, we discuss the path loss prediction for each set of heuristic UTD coefficients in outdoor environment, as well as the comparison with the canonical results.

1. Introduction

The current state of wireless technology, particularly in the urban environment, requires methods to estimate, with high precision, the multipath propagation of wideband radio channels and to minimize the error of on-site measurements. Physical and numerical methods of ray tracing and uniform theory of diffraction (UTD) coefficients are precise and efficient in simulating the path loss in complex environments. The choice of diffraction coefficients is critical for predicting the diffraction signal amplitude. By comparing high-precision and approximate solutions for the diffraction coefficients in canonical problems, as well as in real environments, general observations can be made regarding the ray methods and UTD coefficients.

Ray tracing is one of the most used deterministic technique for propagation prediction. This technique is based in the launching of millions of optical rays. This set of rays interact with the obstacles of the environment modeling the multipath propagation. Each ray is unique and is analyzed individually; then its amplitude and direction is unpredictable due to the multiple diffraction and reflections. Therefore, the numerical methods used to estimate the electromagnetic fields must be robust and accurate for all types of conditions.

The UTD is an asymptotic solution largely used to predict scattering propagation in urban environments. The diffraction occurs when a ray encounters a wedge, which generates multiple new rays determined by a diffraction cone according to the Huygens principle.

The UTD formulation is rigorous because the diffraction coefficients and angular definitions are quite complex and have many exceptions, depending on the wedge geometry and the positions of the transmitter and receiver. Many

heuristic coefficients have been proposed to solve this problem, and the first UTD coefficients were developed for perfectly conducting wedges [1].

Malyuzhinets developed a high-precision solution for wedge diffraction in non-perfectly conducting surfaces [2]. However, the proposed solution is not practical for predicting the propagation in real (complex) environments because it uses a special function that is difficult to calculate numerically for arbitrary wedge angles, but it is a useful reference to compare other numerical solutions.

Luebbers was one of the first to establish heuristic diffraction coefficients for lossy conducting wedges [3]. Luebbers' formulation is very practical in the calculation of the diffracted field but has some problems. It does not obey the reciprocity in relation to the incident field on the wedge, and it is inaccurate in the shadow regions.

Schettino et al. [4] proposed heuristic UTD coefficients by combining features of previous studies [3, 5–7], ensuring reciprocity, and providing superior performance for arbitrary sources and observers' locations. Although good results were obtained, the approach is quite complex because the angular definitions used have many conditions in relation to directions of the incident and diffracted waves.

All these studies present good results but have difficulties, due to either inaccuracy in the shadow regions or complexity in the implementation or difficulty to be applied in large urban scenarios. Aiming at the applicability and efficiency yield, we proposed and implemented a novel approach called Guevara coefficients, which are based on Luebbers' formulation with the addition of a physical method to model the wedge conditions and ensure reciprocity, without depending on the source and observer positions. The main advantage of the Guevara coefficients is the simplicity in the computational implementation for all situations in relation to the position of the incident and diffracted waves. Such a practical approach improves the simulation time when the radio channel prediction is made in complex urban scenarios.

Previous work has shown that the Luebbers, Schettino, and Guevara coefficients can be used to accurately estimate the path loss in real outdoor environments [8–11], but such works were oriented to the evaluation of the implemented tools in real scenarios against measurements. Thus, the objective of this work is to evaluate the reciprocity and accuracy of these three heuristic UTD coefficients suited to characterize the electromagnetic scattering in realistic urban scenarios and compare with canonical examples.

Canonical scenarios are useful to analyze closed-form solutions, as well as numerical implementations in reference well-known and controlled scenarios, including only the diffraction effect. On the other hand, real scenarios are useful to analyze the computational behavior of the numerical implementations as well as the accuracy of such implementations in complex not controlled scenarios, including not only diffraction but also reflections and combinations of such phenomena.

Although different works have been published, the analysis of these models in canonical scenarios, as well as in real scenarios, up to the best knowledge of the authors, is a novel contribution, given that no previous work has shown a comparison between the three approaches in both real and canonical scenarios.

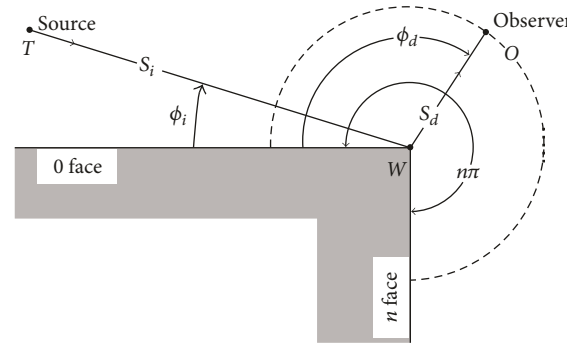

Figure 1: Geometry and wedge diffraction variables.

To evaluate the effectiveness of the three UTD coefficients, we investigated the scattering by arbitrary lossy conducting wedges. The results are compared to the Malyuzhinets solution. Then, the Luebbers, Schettino, and Guevara coefficients are used to estimate the path loss in outdoor environments by using a 3D ray-tracing model based on a brute-force algorithm for ray launching and a propagation model based on image theory. Both models are used to simulate multiple paths, and then, we evaluate the deviation between model estimates and measured data in urban environments.

The paper is organized as follows: in Section 2, we show the results of the general concepts for each one of the coefficients used in the paper; in Section 3, we show the results for the canonical scenarios and compare results; in Section 4, we describe the realistic outdoor scenarios; in Section 5, we describe the propagation models where the heuristic models have been implemented. In Section 6, we show the results of the heuristic coefficients applied to the real outdoor scenarios and compare results. Finally, in Section 7, we present our conclusions.

2. The Malyuzhinets Solution and Heuristic UTD Coefficients

We considered the two-dimensional problem of diffraction by a semi-infinite wedge with straight edges, exterior angle $n\pi$, and lossy conducting boundary surfaces in a homogeneous, linear, and isotropic medium. In the chosen coordinate system, the straight edge of the wedge is along the z-axis, the plane faces of the wedge are at $\varphi = 0$ (0 face) and $\varphi = n\pi$ (n face), the radio source is at $\varphi = \phi_i$ and distance $\rho = s_i$ from the edge of the wedge, and the observation point is at (s_d, ϕ_d). The geometry of the problem is shown in Figure 1.

Malyuzhinets [12] chose the form used by Sommerfeld for a perfectly conducting wedge. Specifically, the entire field at the wedge is expressed as a Sommerfeld integral bounded by the face impedances. The solution to the Malyuzhinets problem is

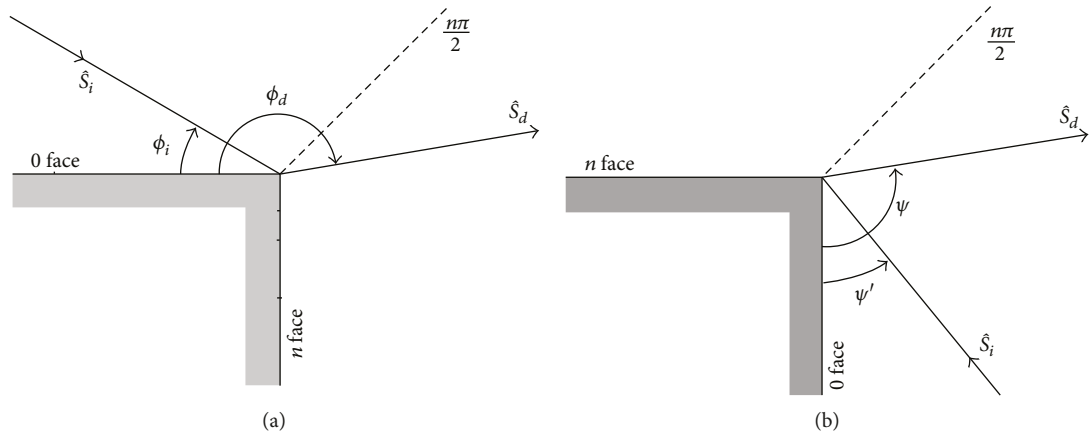

Figure 2: Angular definitions used in Guevara's coefficients.

$$E_z^d = \frac{e^{-jks_d}}{\sqrt{s_d}} D^{nu}(\phi_d, \phi_i), \tag{1}$$

where

$$D^{nu}(\phi_d, \phi_i) = \frac{e^{-j\pi/4}}{n\sqrt{2\pi k}} \frac{\cos(\phi_i/n)}{\psi(\phi_i)} \cdot \left[\frac{\psi(\phi_d - \pi)}{\sin((\phi_d - \pi)/n) - \sin(\phi_i/n)} - \frac{\psi(\phi_d + \pi)}{\sin((\phi_d + \pi)/n) - \sin(\phi_i/n)} \right] \tag{2}$$

is the nonuniform diffraction coefficient, and $\psi(\alpha)$ is a function that depends on Malyuzhinets function and can be evaluated in closed form for special cases [2].

The general UTD solution for the electric field at the observer's point is

$$E_d(O) = E_i(W) \cdot \bar{D} A(s_d) e^{-jks_d}, \tag{3}$$

where $E_i(W)$ is the incident electric field at the wedge, $A(s_d)$ is the amplitude, s_d is the distance between the wedge and the observer, and $\bar{D}$ is the dyadic diffraction coefficient. Adopting the classical notation of [1], the dyadic soft and hard coefficients are

$$\bar{D}^{s,h} = G_0^{s,h} \left[D_2 + R_0^{s,h}(\alpha_0) D_4 \right] + G_n^{s,h} \left[D_1 + R_n^{s,h}(\alpha_n) D_3 \right], \tag{4}$$

where D_i, for $i = 1, \ldots, 4$, are UTD diffraction coefficients, G_0 and G_n are grazing incidence factors, and R_0 and R_n are Fresnel reflection coefficients for the 0 and n faces, respectively. We evaluate three heuristic UTD coefficients to characterize the radio channel.

2.1. Luebbers' Coefficients [3]. They introduced the Fresnel reflection coefficients in the UTD formulation, defining the incidence and reflection angles of the incident and diffracted rays. Although the coefficients are practical, they present difficulties associated with reciprocity and shadow regions because they are derived for forward scattering assuming $\phi_i < \phi_d$. Luebbers' definition for the angles α_0 and α_n, used in the Fresnel reflection coefficients, are

$$\begin{aligned} \alpha_0 &= \phi_i, \\ \alpha_n &= n\pi - \phi_d. \end{aligned} \tag{5}$$

2.2. Schettino's Coefficients [4]. They are proposed as heuristic UTD coefficients based on Holm's formulation [5], with angular definitions for α_0 and α_n based on [6, 7]. In essence, this formulation combines the characteristics of Holm's coefficients [5] with rigorous angular definitions based on the boundary of reflected rays. When only one of the wedge faces, 0 or n, is illuminated, the angular definitions proposed in [7] are adopted, but when both faces are illuminated, the angular definitions proposed in [6] proved to be more appropriate. The full description of these definitions can be found in [4]. Although Schettino's coefficients ensure reciprocity and achieve better results for arbitrary source and observer locations, they are not practical to be applied in large urban scenarios, because of their computational complexity.

2.3. Guevara's Coefficients. They are based on Luebbers' formulation [3], adopting novel angular definitions for ψ' and ψ to obey the reciprocity and a physical method which allow modeling the diffraction at the side edges of buildings. They also allow the characterization of the building walls and roofs and street pavements using common dielectric parameters for each group in real scenarios.

Figure 2 shows the novel angular definitions in Guevara coefficients. If the incident ray is in the region defined by $\phi_i \leq (n\pi)/2$, the ϕ_i and ϕ_d angles are maintained equal to Luebbers (see Figure 2(a)), but if the incident ray arrives in the region $\phi_i \geq (n\pi)/2$, the face assignments are exchanged, see Figure 2(b), and Luebbers' conditions are applied defining

$$\begin{aligned} \phi_i &= \psi', \\ \phi_d &= \psi. \end{aligned} \tag{6}$$

With ϕ_i and ϕ_d defined above, the Fresnel reflection coefficients, $R_0(\alpha_0)$ and $R_n(\alpha_n)$ for the 0 and n faces, respectively, are calculated with

$$\begin{aligned} \alpha_0 &= \phi_i, \\ \alpha_n &= \min[\phi_d, n\pi - \phi_{\mathrm{d}}]. \end{aligned} \tag{7}$$

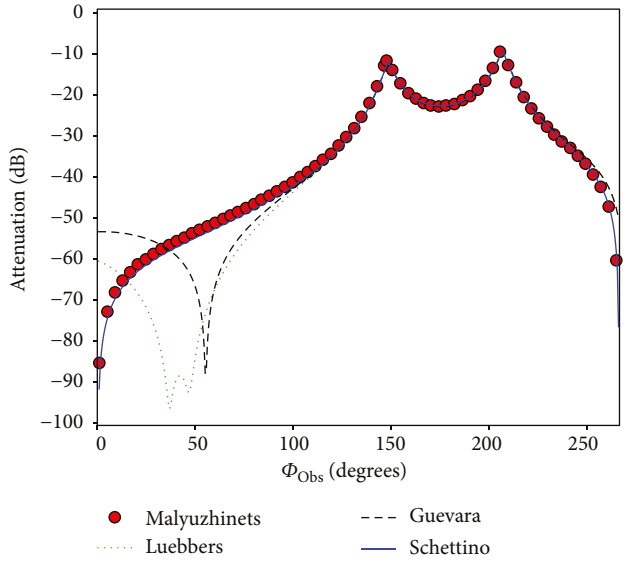

Figure 3: Attenuation of the diffracted field for TM polarization around the wedge; 0-face incidence and $\phi_i = \pi/6$.

3. Canonical Analysis of Diffraction by Lossy Conducting Wedges

Conventional geometric shapes can be used to model most buildings in urban environments (e.g., buildings can be modeled as orthogonal parallelepipeds). Hence, we study the diffraction on a lossy wedge with 90° internal angle, and $\epsilon_r = 10$ and $\sigma = 0.01$ S/m. The wedge is illuminated by a normally incident plane wave at 1 GHz (Figure 1). Three types of incidence are analyzed, zero-face incidence, n-face incidence, and incidence on both faces for $\phi_i = \pi/6$, $(3\pi)/4$, and $(4\pi)/3$, respectively. We also compare the results using the three sets of heuristic coefficients, that is, Luebbers, Schettino, and Guevara. In the analysis, TM (soft) and TE (hard) polarizations are considered and the Malyuzhinets coefficients [6] are adopted as reference. The observer is at 30λ from the edge for $0 \le \phi_d \le (3\pi)/2$. Although the common usage in the literature for canonical scenarios is the field strength representation, in the following figures, we will use the relative attenuation expressed in dB, because of its common use in real scenarios and measurements. This representation does not modify the meaning of the results and the conclusions.

Figures 3 and 4 show the relative attenuation of the diffracted field ($|E_d/E_i|$) in dB for 0-face incidence and $\phi_i = \pi/6$ for the TM and TE polarizations, respectively. Table 1 lists the mean and standard deviation (SD) of the absolute error.

Figures 5 and 6 show the attenuation of the diffracted field for incidence on both faces at $\phi_i = (3\pi)/4$ for TM and TE polarizations, respectively. Table 2 lists the mean and standard deviation of the absolute error.

Figures 7 and 8 show the attenuation of the diffracted field for incidence on the nth face at $\phi_i = (4\pi)/3$ for TM and TE polarizations, respectively. The incidence angle of the plane wave represents the reciprocity case at $\phi_i = \pi/6$.

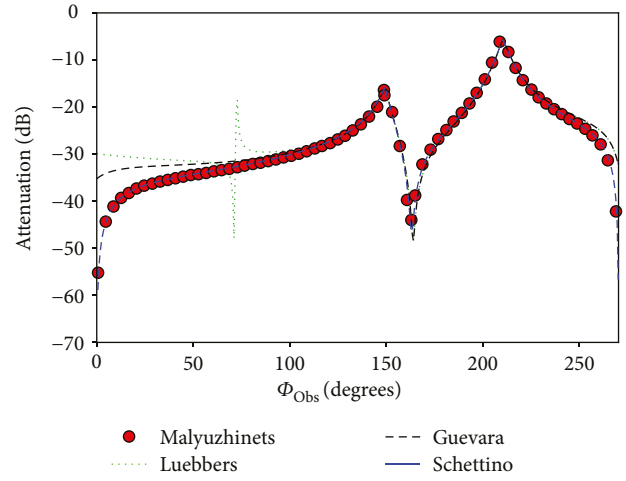

Figure 4: Attenuation of the diffracted field for TE polarization around the wedge; 0-face incidence and $\phi_i = \pi/6$.

Table 1: Statistics for the 0-face incidence.

UTD coefficients	TM polarization		TE polarization	
	Mean (dB)	SD (dB)	Mean (dB)	SD (dB)
Luebbers	6.40	10.41	3.22	4.58
Guevara	4.11	6.65	2.47	3.55
Schettino	0.67	0.55	0.49	0.52

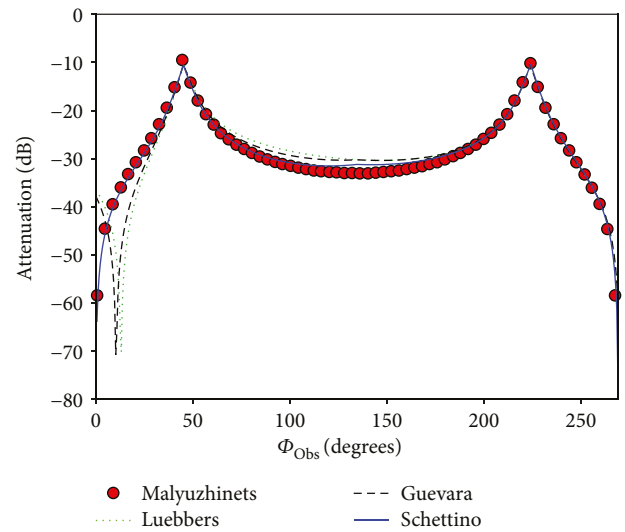

Figure 5: Attenuation of the diffracted field for TM polarization around the wedge; incidence on both faces at $\phi_i = (3\pi)/4$.

Table 3 lists the mean and standard deviation of the absolute error. In this case, the difference between the Luebbers and Guevara models, which includes an adjustment to incorporate reciprocity, is significant. For the TE polarization, Guevara's model behaves like Schettino's and Malyuzhinets' solutions, coinciding with the reciprocity included in Guevara's model. As shown in Table 3, Guevara's model outperforms the Luebbers model in both polarizations.

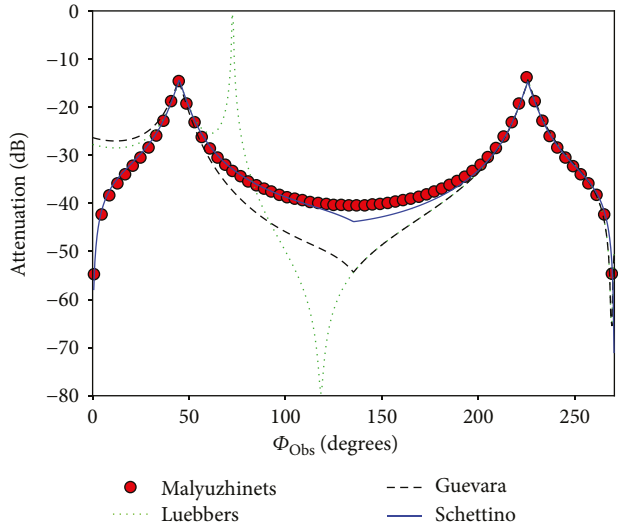

Figure 6: Attenuation of the diffracted field for TE polarization around the wedge; incidence on both faces at $\phi_i = (3\pi)/4$.

Table 2: Statistics for incidence on both faces.

UTD coefficients	TM polarization		TE polarization	
	Mean (dB)	SD (dB)	Mean (dB)	SD (dB)
Luebbers	2.85	4.88	6.62	8.16
Guevara	2.24	3.31	4.83	4.91
Schettino	0.69	0.57	0.97	0.87

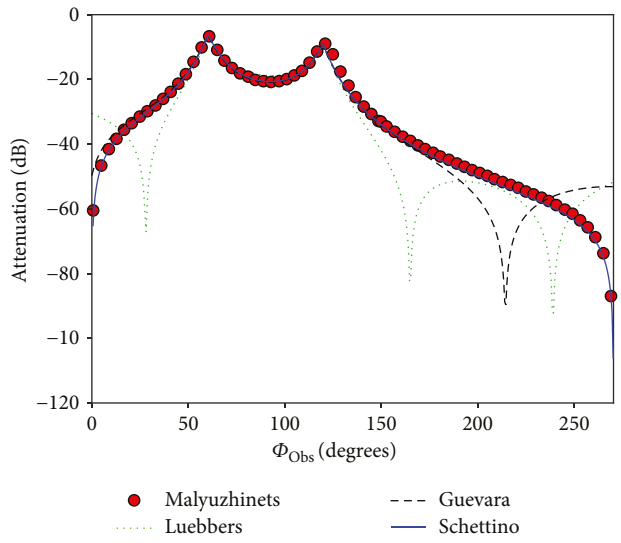

Figure 7: Attenuation of the diffracted field for TM polarization around the wedge; n-face incidence at $\phi_i = (4\pi)/3$.

We observe that the Schettino coefficients offer higher precision than the Guevara and Luebbers solutions for the canonical scenarios. The Luebbers and Guevara coefficients yield inaccurate predictions of the diffracted field. The inaccuracies are in the deep shadow regions (e.g., initial $\phi_d < \pi/2$ for the 0-face incidence and final $\phi_d > (5\pi)/6$ for the n-face incidence), in good agreement with literature.

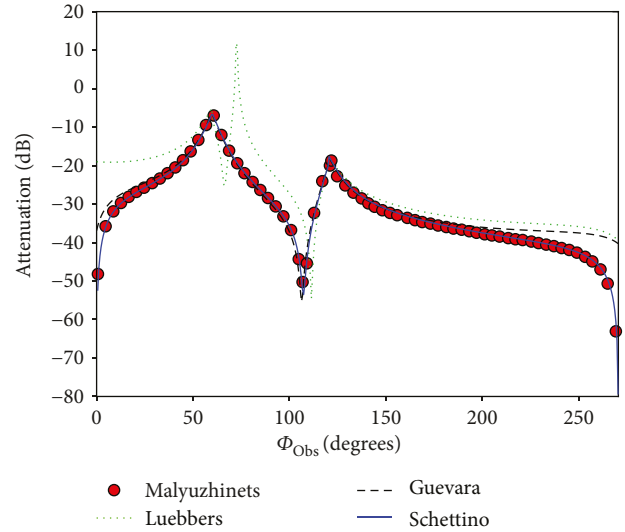

Figure 8: Attenuation of the diffracted field for TE polarization around the wedge; n-face incidence at $\phi_i = (4\pi)/3$.

Table 3: Statistics for n-face incidence.

UTD coefficients	TM polarization		TE polarization	
	Mean (dB)	SD (dB)	Mean (dB)	SD (dB)
Luebbers	7.64	8.41	6.53	5.40
Guevara	4.39	6.81	2.45	3.58
Schettino	0.87	0.82	0.48	0.52

4. Realistic Outdoor Scenarios

The aim of most implementations of diffraction coefficients using ray-based models is the use as deterministic models in real scenarios for wireless network planning. It is expected that ray-based models will be useful for the planning of 4G/5G networks, not only because of their higher precision in predicting path loss but also because of their capacity to predict channel parameters. We implemented the three different coefficients in three different realistic urban scenarios, which will be described next.

4.1. Ottawa City, Canada [8]. The urban scenario is a typical downtown area of 0.6 km × 0.9 km with complex building architecture. The propagation model is a 3D ray-tracing model in C++. The 3D model is based on image theory and considers reflections from streets and building faces and diffraction on building edges. Neither reflections nor diffractions at the building tops are considered.

Figure 9 shows the simulation and data collection routes (blue line for Bank St. and red lines for Laurier St., Slater St., and Queen St.). The radio signal at 910 MHz is supplied by a transmitter (Tx) at 8.5 m height (blue point for Bank St. and red point for Laurier St., Slater St., and Queen St.). The propagation losses were obtained by measuring the power in the selected routes. The mobile receiver antenna is fixed on the top of the test car at 3.65 m above the ground; 291 and 452 measurements were collected along the streets [13].

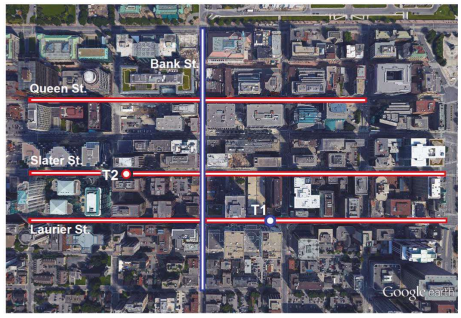

Figure 9: Downtown Ottawa City, Canada, from Google Earth.

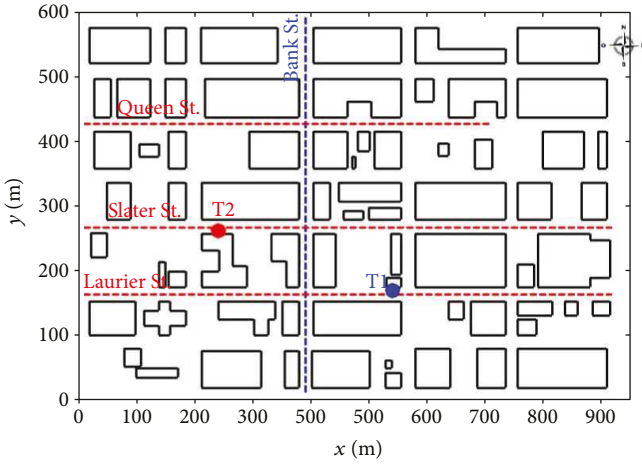

Figure 10: The 2D urban model of Ottawa, Canada.

Figure 10 shows a 2D model of downtown Ottawa City. The streets and buildings are modeled by using flat polygons. To take into account the effects of diffraction on channel response, we model the building edges as points at the vertices of each polygon. The number of buildings in the model is 68. We also assumed $\varepsilon_r = 7$ and $\sigma = 0.2$ S/m for the reflections and diffractions from buildings and $\varepsilon_r = 15$ and $\sigma = 0.05$ S/m for the reflections from the streets [14]. In addition, Figure 9 shows the routes taken in each case. The measurements along these routes were used to evaluate the propagation models with the heuristic UTD coefficients.

4.2. Cali, Colombia [9]. This is an urban microcell 512 m × 512 m, with strongly inclined roads and complex building architecture of different heights (see Figure 11).

Figure 12 shows the 3D urban model for the Cost2100 Cali Realistic Scenario with 1 m resolution. We used a 3D model to represent the streets, roofs, and walls of buildings. The number of buildings in the model is 400 [15].

The data collection campaign involved collecting the power received in a specific route at street level around the transmitter (see green spheres in Figure 12). The transmitter antenna produced a signal at 900 MHz and was located on the top of a building at 16 m above it (see blue object in Figure 12). The receiver system consisted of a low-profile mobile and vertically polarized antenna mounted on the test car, and the receiver antenna was positioned above the center

Figure 11: Downtown Cali City, Colombia, from Google Earth.

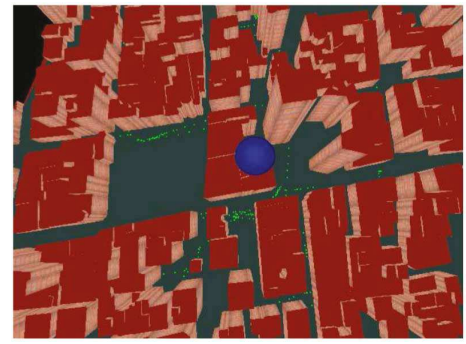

Figure 12: 3D urban model for Cali using a game engine.

Figure 13: Universitat Politècnica de València from Google Earth.

of the vehicle roof at 2.1 m above the ground; 258 measurement points were collected [16].

4.3. Valencia, Spain [10]. This is a suburban macrocell in the main campus of the Universitat Politècnica de València (UPV). Figure 13 shows the simulation and data collection route (green line). This is a 2 km × 2 km area, with slightly inclined roads and complex building architecture. A digital video broadcasting (DVB) signal at 496 MHz was produced by a transmitter (Tx) on the top of a building in the main campus at 24 m height (red point in Figure 13).

Data were obtained during a data collection campaign that measured the power received at street level, inside and outside the campus, and around the transmitter. The receiver system consisted of a TeamCast professional receiver with a vertical quarter-wavelength monopole, a GPS, and software to collect and store the data. This system was in a test car with a receiver antenna on the top of the vehicle; data were collected at 1380 points in the drive test [8].

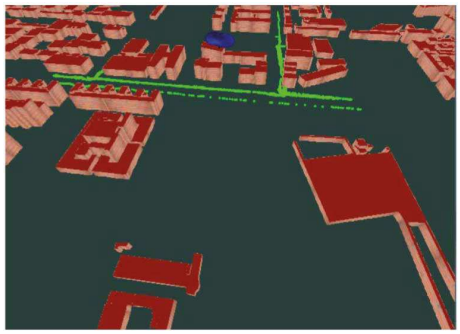

Figure 14: Localization of the receiver points with LOS and NLOS (green spheres) and the transmitter (blue).

Figure 14 shows a 3D digital terrain model (DTM) of Valencia. The DTM was recreated using the jMonkeyEngine (jME v2.0). We modeled the streets, roofs, and walls of buildings by using spatial geometries. Additionally, Figure 14 shows the data collection route identified by the green spheres, which represent the reception points in the middle of the streets.

For the scenarios of Cali and Valencia, a propagation model based on 3D ray launching by "brute-force," also known as shooting and bouncing ray (SBR), algorithm was used. The scenario was built using a 3D urban model supported in jMonkeyEngine and graphics processing unit (GPU) [17]. The number of interactions (reflections, diffractions, and combinations) used to model the multipath propagation was limited to five combinations in total. The number of diffractions is limited to two, and the number of reflections considered is up to five. The experience has shown that a number of five wave interactions (reflection and diffraction) are sufficient to obtain a good accuracy with respect to measurements and obtain an adequate efficiency in processing time [18]. Most of the buildings and street materials in the two cities have the same constitutive parameters (i.e., permittivity, permeability, and rugosity). Specifically, we assumed brick ($\varepsilon_r = 7\text{-}j0.3$, $\mu_r = 1$) for all building walls, a first type of dry concrete ($\varepsilon_r = 5.3\text{-}j0.25$, $\mu_r = 1$) for all building roofs, and a second type of dry concrete ($\varepsilon_r = 7\text{-}j0.3$, $\mu_r = 1$) for street pavement [17].

The radio channel measurement in the three scenarios characterized the propagation loss for the routes, which include localizations with LOS and NLOS.

5. Propagation Models

We have used a 3D ray-tracing model to the Canada urban scenario. It is supported in C++. This propagation model is based on image theory (IT). In principle, IT is more rigorous than brute-force algorithm, as the former can determine all ray-path components—including diffracted rays—without redundancies. The IT uses optical images of the transmitter and diffraction points, considering the obstacle surfaces as reflectors. The environment of the urban scenario will be represented by an approximate model: the obstacles are modeled as polygons with finite heights and placed perpendicularly over a flat ground [11].

Table 4: Software and hardware requirements.

Software	Operating system	Windows 7-64 bits
	Programming language	Java
	IDE	Eclipse
	Application programming	Open Graphics Library (OpenGL)
	Java native interface binding to	Lightweight Java Game Library
	Graphics engine	Java Monkey Engine (jME) v2.0
	Physics engine	Open Dynamics Engine (ODE)
	jME interface to ODE	jME Physics 2
	GIS toolkits	GeoTools
Hardware	Processor	Intel® Xeon® 2x 8-Core, 2.6 GHz
	RAM memory	16 GB
	GPU	NVIDIA Quadro 4000

Here, we used a ray-tracing algorithm, where direct, reflected, and diffracted components are considered. Ray paths are then formed from combinations among those components, with a maximum number of reflections, $N_R = 5$, and diffractions, $N_D = 5$. Initially, a 2D algorithm traces the trajectories. The 2D rays are then converted into 3D ones. Each 2D path between T and R generates two 3D trajectories: one that reflects once at the ground reaching R and another that does not. In the process, reflections from the ground and the finite heights of buildings are appropriately accommodated [11]. The hardware used was a desktop with Intel core i5 processor of 3.46 GHz clock speed and 8 GB RAM, equipped with a basic GPU.

On the other hand, we have used another propagation model to the Cali and Valencia urban scenarios. It is a 3D ray-tracing model based on a brute-force algorithm for ray launching. It is supported in Java Monkey Engine (jME) v2.0. Table 4 shows a summary of the software and hardware requirements for this propagation model. It is important to note that some physical effects of ray launching are managed by Open Dynamics Engine (ODE) that is a specialized tool for effects like bouncing, collision detection, and other dynamic effects. Additionally, ODE implements also the ray physics that interoperates with the jME's ray tracing.

The core of ray launching is the test intersection between a ray and the world bounds. We used the GPU computational capacity to estimate the interaction of ray with all the bounds in the database compute. The ODE engine builds the bouncing model. This model avoids increasing the total running time and memory of the central processing unit (CPU). The CPU is used to compute the ray-launched parameters or the family of new rays to its next object and so on. This task demands more computational time compared to estimating the interaction of the ray. The jME engine is used to build the 3D model, to implement the ray-launching process, and to visualize results. The implemented propagation model supports full 3D diffraction.

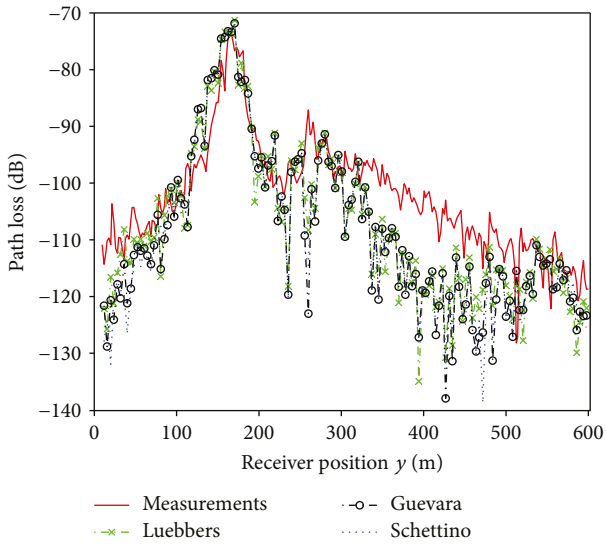

FIGURE 15: Path loss comparison between the heuristic UTD coefficients and data (red line) for Bank St.

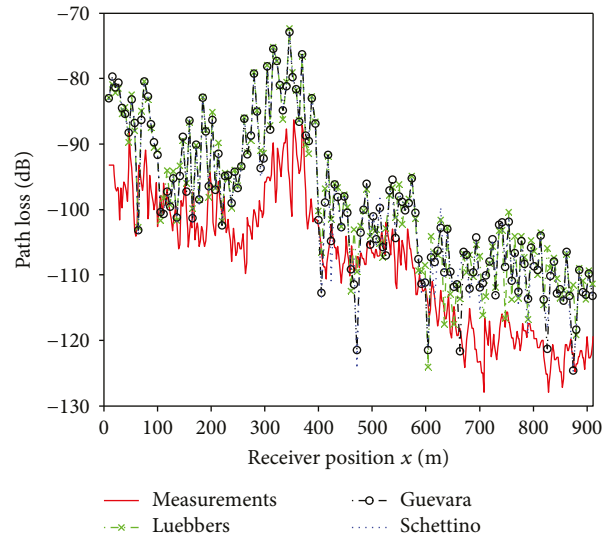

FIGURE 16: Path loss comparison of model and measured data (red line) for Laurier St.

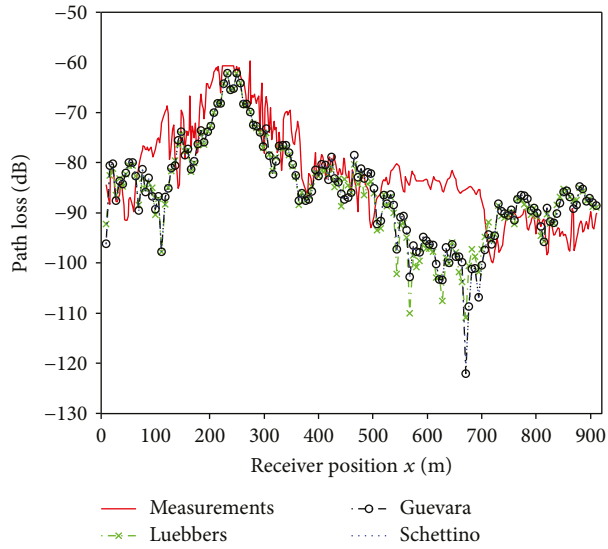

FIGURE 17: Path loss comparison of model and measured data (red line) for Slater St.

The ray launching models radio waves as optic rays that follow a straight path from transmitter to receiver. During this process, the wave interacts with bounding box that represents walls, roofs, streets, bounding spheres for the receiver, and bounding cylinder for the building edge. In order to model the reflection phenomena in walls, roofs, and streets, we apply the rugosity factor to calculate the reflection coefficients. In order to model diffractions in corners and edges of buildings, we apply UTD and the three sets of heuristic coefficients. Through this process, we obtain all possible multipath components between the transmitter and receiver. Once we have obtained multipath tracing for each Tx-Rx pair, we know the parameter wave attenuation, depolarization, phase shift, delay, angle of arrival, and angle of departure. Therefore, we obtained a visibility tree for all relevant multipath components.

In order to compute the diffracted rays, we used shooting and bouncing launching algorithm with a mean angular separation, $\alpha_d \approx 0.135^\circ$, between neighbour rays in 3D space. When a ray hits on an edge, the program models the diffraction phenomenon, producing a source of new rays determined by a diffraction cone and an angular resolution, α_d for the first diffraction and $2\alpha_d$ for the second. In the next step, each diffracted ray can hit on flat polygons, reception sphere, or edge cylinder, determining the values for the angles ϕ_i and ϕ_d. After, it checks angular definitions used according to the formulations given and Luebbers', Schettino's, and Guevara's coefficients. Finally, the UTD is applied to asymptotically evaluate the electromagnetic field associated with each multipath component for each heuristic coefficients.

6. Results and Discussion

The first simulated scenario is Ottawa. The results for Bank St., Laurier St., Slater St., and Queen St. routes are shown in Figures 15–18, respectively. Observe that Slater St. is mainly a LOS scenario, whilst Bank St., Laurier St. and Queen St. are mainly NLOS scenarios, with high influence of diffractions.

Table 5 summarizes the mean absolute error (MAE) and standard deviation of the absolute error (SD) for each Ottawa route.

The statistical analysis shows that, for the four routes, the three coefficients produce similar results. For Laurier St., Slater St., and Queen St., Guevara's and Schettino's coefficients produce slightly better results but without statistical significance.

The results for Cali are shown in Figure 19.

Table 6 lists the mean and standard deviation of the absolute error to Cali predictions.

In the Cali scenario, Luebbers' coefficients yield slightly better results; however, the difference with the other heuristic

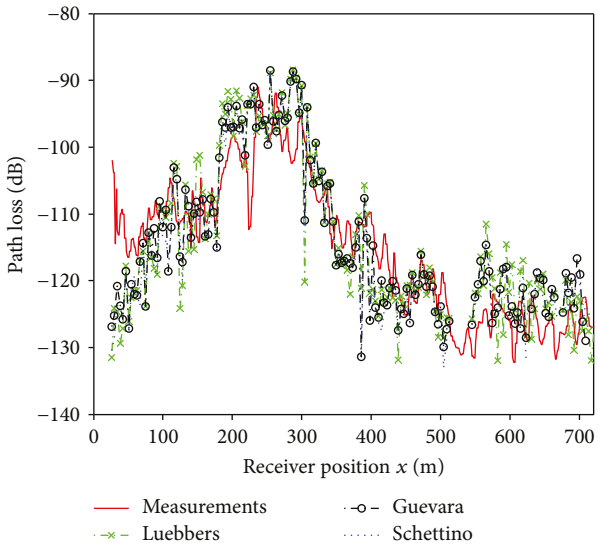

Figure 18: Path loss comparison of model and measured data (red line) for Queen St.

Table 5: Statistics of the path loss for Ottawa City.

UTD coefficients	Bank St.		Laurier St.		Slater St.		Queen St.	
	MAE (dB)	SD (dB)	MAE (dB)	SD (dB)	MAE (dB)	SD (dB)	MAE (dB)	SD (dB)
Luebbers	7.41	5.77	9.94	6.09	7.00	5.92	5.55	4.51
Guevara	8.27	6.35	9.51	5.19	6.98	5.55	5.23	4.46
Schettino	8.33	6.20	9.48	5.17	6.99	5.54	5.18	4.43

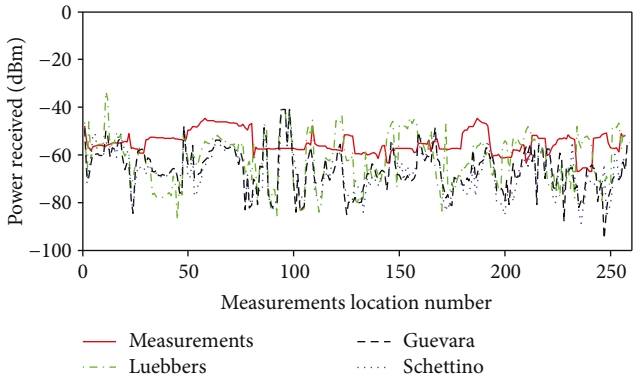

Figure 19: Comparison of model and measured power data for Cali City.

formulations is small. From Figure 19, we can see that Guevara's and Schettino's coefficients have a very similar behavior, differing from Luebbers' behavior, because of the reciprocity condition included by Guevara.

For the Valencia scenario, the results to the set of coefficients are shown in Figure 20.

Table 7 lists the mean and standard deviation of the absolute error to Valencia predictions.

In the case of Valencia, the Guevara coefficients have the smallest mean absolute error and standard deviation;

Table 6: Statistics of the path loss for Cali City.

UTD coefficients	Mean absolute error (dB)	Standard deviation (dB)
Luebbers	8.76	5.75
Guevara	11.25	5.36
Schettino	11.73	5.56

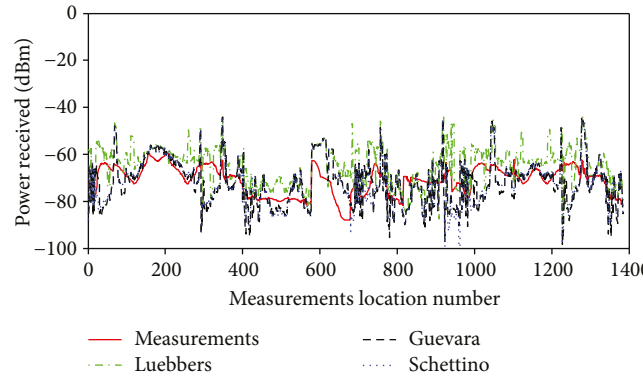

Figure 20: Comparison between ray tracing using the heuristic UTD coefficients and data (red line) for the city of Valencia.

Table 7: Statistics of the path loss prediction for Valencia.

UTD coefficients	Mean absolute error (dB)	Standard deviation (dB)
Luebbers	5.51	7.96
Guevara	4.79	5.95
Schettino	5.08	6.02

however, the differences with Schettino's coefficients is small. In contrast, the difference with Luebbers' coefficients is a bit higher (SD > 2 dB). From Figure 20, we can see that the behavior of the Guevara and Schettino implementations are similar and differ from Luebbers'.

The Guevara coefficients are obtained by appropriately modifying Luebbers' coefficients. The canonical analysis of the diffraction at lossy conducting wedges suggests that all sets of coefficients yield similar results, but Schettino's coefficients are more accurate. However, the Luebbers coefficients do not address reciprocity, whereas the Schettino and Guevara coefficients do.

The agreement between the predictions for the path loss is more notable in the case of Ottawa, where the 3D ray-tracing propagation model based on image theory was applied, and less so for Cali and Valencia, where a 3D ray-tracing propagation model based on a brute-force algorithm or ray launching, including diffractions over rooftops, was applied. In real scenarios, differences in results between the three different implementations are small and possible differences will be in computational time.

The results suggest that it is better to use the Guevara coefficients to predict the path loss in outdoor environments because this solution is more practical to implement

in all situations in relation to the position of the incidence and diffraction. Therefore, it improves the applicability and efficiency in the computational simulations. All case studies indicated the usefulness and applicability of Guevara's coefficients to radio channel prediction in complex urban scenarios.

7. Conclusions

We discussed the implementation and results of the Luebbers, Schettino, and Guevara UTD coefficients, to predict the path loss in outdoor environments by using two propagation tools using ray-based models, as well as in canonical scenarios. We simulated multiple paths and evaluated the absolute error for the three sets of coefficients, showing the differences between the heuristic coefficients in both canonical and real scenarios.

Good agreement was found between the predictions obtained with the Guevara and Schettino coefficients. It is important to note that Guevara's coefficients are a novel practical approach suited to assure reciprocity, despite source and observer positions, and consequently, they can be widely used for the characterization of radio channels in urban scenarios.

Selected outdoor environments were sufficiently diverse, both in the geometry and in frequency, to guarantee statistically representative results to compare the behavior of the three implemented heuristic UTD coefficients. Reciprocity considerations are important from the point of view of computational complexity and behavior in canonical scenarios but has a negligible impact on the results in real outdoor scenarios.

The behavior of the coefficients is different in real scenarios and in canonical scenarios, probably because of the stochastic nature of the ray behavior in real scenarios, which in average avoids the angles where the specific model does not have good performance or because direct trajectories prevail.

In canonical scenarios, the Luebbers model has the worst behavior, as expected, but the difference is negligible in real scenarios, explaining its popularity in different simulation tools.

The prediction results are more remarkable for the propagation method based on the SBR algorithm. The consideration of reciprocity is negligible to the simulated real outdoor environments, because the direct trajectories seem to prevail.

The mean absolute error is high because propagation models based in ray-tracing techniques are deterministic and highly dependent on the accuracy of the modelled scenario. For future 5G systems, higher precision is required, and thus, further analysis of the constitutive parameters is needed.

Conflicts of Interest

The authors declare that they have no conflicts of interest.

Acknowledgments

This work was supported by CNPq and CAPES, Brazil. The authors would like to thank iTEAM and Professor Narcis Cardona for their help in Valencia.

References

[1] R. Kouyoumjian and P. Pathak, "A uniform geometrical theory of diffraction for an edge in a perfectly conducting surface," *Proceedings of the IEEE*, vol. 62, no. 11, pp. 1448–1461, 1974.

[2] T. Senior and J. Volakis, *Approximate Boundary Conditions in Electromagnetics*, IEEE, London, 1995.

[3] R. Luebbers, "A heuristic UTD slope diffraction coefficient for rough lossy wedges," *IEEE Transactions on Antennas and Propagation*, vol. 37, no. 2, pp. 206–211, 1989.

[4] D. Schettino, F. Moreira, and C. Rego, "Heuristic UTD coefficients for electromagnetic scattering by lossy conducting wedges," *Microwave and Optical Technology Letters*, vol. 52, no. 12, pp. 2657–2662, 2010.

[5] P. Holm, "A new heuristic UTD diffraction coefficient for nonperfectly conducting wedges," *IEEE Transactions on Antennas and Propagation*, vol. 48, no. 8, pp. 1211–1219, 2000.

[6] M. Aïdi and J. Lavergnat, "Comparison of Luebbers' and Maliuzhinets' wedge diffraction coefficients in urban channel modelling," *Progress In Electromagnetics Research*, vol. 33, pp. 1–28, 2001.

[7] H. El-Sallabi and P. Vainikainen, "Improvements to diffraction coefficient for non-perfectly conducting wedges," *IEEE Transactions on Antennas and Propagation*, vol. 53, no. 9, pp. 3105–3109, 2005.

[8] D. Tami, C. Rego, D. Guevara, A. Navarro, and F. Moreira, "Heuristic UTD coefficients for radiowave coverage prediction in a urban scenario," in *2015 SBMO/IEEE MTT-S International Microwave and Optoelectronics Conference (IMOC)*, Porto de Galinhas, Brazil, November 2015.

[9] D. Tami, C. Rego, F. Moreira, D. Guevara, and A. Navarro, "Heuristic UTD coefficients applied for the channel characterization in an Andean Scenario," in *2015 IEEE International Symposium on Antennas and Propagation & USNC/URSI National Radio Science Meeting*, Vancouver, BC, Canada, July 2015.

[10] D. Tami, C. Rego, D. Guevara et al., "Comparison of heuristic UTD coefficients in an outdoor scenario," in *2015 9th European Conference on Antennas and Propagation (EuCAP)*, pp. 1780–1784, Lisbon, Portugal, April 2015.

[11] D. Schettino, F. Moreira, and C. Rego, "Efficient ray tracing for radio channel characterization of urban scenarios," *IEEE Transactions on Magnetics*, vol. 43, no. 4, pp. 1305–1308, 2007.

[12] D. Malyuzhinets, "Excitation, reflection and emission of surface waves from a wedge with given face impedances," *Soviet Physics – Doklady*, vol. 3, pp. 752–755, 1958.

[13] J. Whitteker, "Measurements of path loss at 910 MHz for proposed microcell urban mobile systems," *IEEE Transactions on Vehicular Technology*, vol. 37, no. 3, pp. 125–129, 1988.

[14] S. Y. Tan and H. S. Tan, "Propagation model for microcellular communications applied to path loss measurements in Ottawa city streets," *IEEE Transactions on Vehicular Technology*, vol. 44, no. 2, pp. 313–317, 1995.

[15] A. Navarro and D. Guevara, "Using game engines for wideband channel estimation parameters in Andean cities," in *2010 Proceedings of the Fourth European Conference on Antennas and Propagation (EuCAP)*, Barcelona, Spain, April 2010.

[16] A. Navarro and D. Guevara, "Applicability of game engine for ray tracing techniques in a complex urban environment," in *2010 IEEE 72nd Vehicular Technology Conference - Fall*, Ottawa, ON, Canada, September 2010.

[17] A. Navarro, D. Guevara, N. Cardona, and J. Lopez, "Measurement-based ray-tracing models calibration in urban environments," in *Proceedings of the 2012 IEEE International Symposium on Antennas and Propagation*, Chicago, IL, USA, July 2012.

[18] K. A. Chamberlin and R. J. Luebbers, "An evaluation of longley-rice and GTD propagation models," *IEEE Transactions on Antennas and Propagation*, vol. 30, no. 6, pp. 1093–1098, 1982.